Journal of
Ceramic Science
and Technology

J. Ceram. Sci. Tech., 04 [02] 51-58 (2013)
DOI: 10.4416/JCST2012-00029
available online at: http://www.ceramic-science.com

Influences of Cation Disorder in Commercial Spinel Powders Studied by ^{27}Al MAS NMR on the Sintering of Transparent $MgAl_2O_4$ Ceramics

A. Krell*[1], E. Brendler[2]

[1]Fraunhofer-Institut für Keramische Systeme und Technologien (IKTS, Fraunhofer Institute for Ceramic Systems and Technologies), 01277 Dresden, Germany
[2]TU Bergakademie Freiberg (Freiberg University of Mining and Technology), Faculty of Chemistry and Physics, 09599 Freiberg, Germany

received August 16, 2012; received in revised form September 21, 2012; accepted October 14, 2012

Abstract

At the Stockholm Conference of the European Ceramic Society 2011 it was shown that, together with the particle size of raw powders and the homogeneity of particle coordination in the green bodies, the real structure of the lattices is a third major influence on sintering, which may differ significantly even at fixed stoichiometry. Antisite defects govern the whole defect chemistry of $MgAl_2O_4$ and should, therefore, affect diffusion and sintering. This possibility is investigated here with solid state ^{27}Al MAS nuclear magnetic resonance measurements of the occupancy of octahedral and tetrahedral sites. Based on previous results with model powders synthesized in order to identify lattice effects at constant particle size distribution, homogeneity and composition, the study has now been extended to commercial spinel powders supplied by Asian, European, and American manufacturers. The results confirm a correlation of increasing cation disorder with improved sintering densification.

Keywords: Spinel ($MgAl_2O_4$), transparency, sintering, antisite defects, ^{27}Al NMR

I. Introduction

Magnesium aluminate spinel is a candidate for sintered windows, domes and lenses for ultraviolet (UV), visible (VIS), and infrared (IR) applications. As in all transparent materials the residual porosity has to be < 0.01 % to ensure high transmittance and a glass-like appearance. This extreme challenge demands raw powders with high sintering activity. At a fixed small particle size < 300 nm, sintering densification is further promoted by processing approaches that improve the homogeneity of the particle coordination in the green bodies. For example, improved processing reduced the sintering temperature of a given Al_2O_3 powder from ~ 1500 °C to < 1300 °C [1] and, later on, to 1130 °C [2]. Evidence of the homogeneity as the origin of this substantial effect came from measurements that showed improved (narrower) pore size distribution in the green bodies [2, 3]. A comprehensive summary of the roles of particle size and of homogeneity has been given previously [4].

Unfortunately, most cubic oxides preferred for transparent ceramics exhibit structures that are not as well-defined and stable as that of, for example, corundum. With only $^1/_8$ of the available tetrahedral sites occupied by Mg^{2+} and $^1/_2$ of the octahedral sites occupied by Al^{3+} species, stoichiometric $MgAl_2O_4$ crystals exhibit a significant propensity for cation exchange and interstitial defects [5]. The degree of cation exchange is described by the inversion parameter *i* defined as the fraction of tetrahedral sites occupied by Al species (AlO_4) [6] or by the expression $(Mg_{1-i}Al_i)[Mg_iAl_{2-i}]O_4$ where the parentheses refer to tetrahedral and the square brackets to octahedral (AlO_6) sites [7]. Such cation disorder must influence diffusion and sintering. Experimental investigations of these correlations are, however, complicated because any sintering body will also be subject to the other (eventually dominating) influences of particle size and homogeneity. Let us address two examples:

- For commercial high-purity stoichiometric $MgAl_2O_4$ spinel powders made by means of flame spray pyrolysis (particle size ~ 50 – 60 nm) or thermal decomposition with ammonium carbonate (particle size ~ 120 nm) and processed such that the shaped green bodies exhibit equal homogeneity (indicated by a 2-fold pore size in the bodies of spinel with 2-fold particle size) [8], the difference of ~ 300 °C in the sintering temperatures (Fig. 1) was clearly dominated by the different sizes of powder particles and pores (20 and 40 nm) in the green bodies.
- Comparing, on the other hand, the flame spray pyrolysis spinel with an alum-process spinel of similar median particle size (50 – 60 nm) the one granulometric difference was a slightly deteriorated homogeneity of shaped green alum spinel bodies with 23 nm median

* Corresponding author: Andreas.Krell@ikts.fraunhofer.de

pore size vs. 20 nm for flame spray pyrolysis [8]. Nevertheless, these samples exhibited a big difference in their sintering temperatures of about 200 °C (Fig. 1) – giving rise to the question whether it was right to attribute the different sintering to the slightly different green body homogeneity only [8] or whether there is some additional other influence behind this observation.

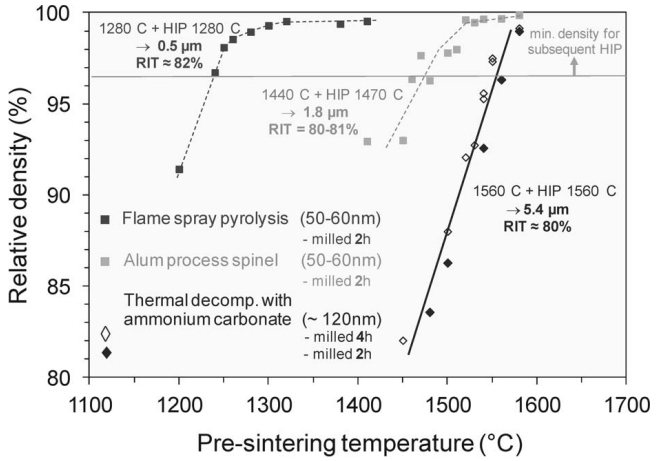

Fig. 1: Pressureless pre-sintering of differently synthesized commercial spinel powders in air (2 h). The inserts give the optimum pre-sintering and HIP temperatures (for maximum transmission of the powder in question), the obtained maximum transmission RIT (at 3 – 4 mm thickness) and the average grain size of these transparent samples [8].

With regard to the highly dynamic character of the flame spray pyrolysis and the static calcination of the alum process, it is most probable that this additional influence could come from different structures of these differently synthesized lattices. A scientifically valid answer cannot be obtained, however, by investigating only commercial powders because no such powders exist which owing to fundamentally different syntheses exhibit significantly different lattices with, nevertheless, equal particle size distributions and equal dispersibility (enabling equal homogeneity of green bodies) as prerequisites for successful separation of the different influences. Such an insight could, however, be obtained by studying laboratory-synthesized stoichiometric spinel powders [9]:

– Two high-purity spinels with similar particle sizes were obtained with basically different approaches. (A): 50 nm MgO particles were dispersed in a solution of an alumina precursor, and after precipitation of the Al component on the surfaces of the MgO particles, drying, calcination at 1100 °C, processing and shaping, the green bodies exhibited a specific surface of 68 m^2/g (equivalent to ~ 25 nm particle size) with extremely fine and narrow pore size distribution (d_{50} ~ 11 nm, d_{95} ~ 12 nm). (B): An almost equal pore size distribution (d_{50} ~ 9.5 nm, d_{95} ~ 11.5 nm) and specific surface (70 m^2/g) was obtained after same processing and calcination starting from a mixture of organic magnesia and alumina precursors [9]. Thus, regarding the constant stoichiometry, the same calcination with constant granulometric parameters, and the constant homogeneity of the shaped green bodies, the powders (A) and (B) were expected to exhibit similar sintering temperatures.
– However, shaped bodies of spinel (A) came to closed porosity (the prerequisite for subsequent cladless hot isostatic pressing [HIP]) at about 1480 °C whereas spinel (B) achieved the same state at 1270 °C – a difference of more than 200 °C [9] ! The one possible explanation was the assumption that building the spinel lattices (A) on a pre-existing cubic template of nanoscale MgO particles or (B) *ab initio* starting with organic precursors and running through amorphous intermediate phases resulted in lattices with different structures. And the most prominent feature of such differences is the cation disorder addressed above when Al species switch from regular octahedral to tetrahedral (Mg-) sites.

For decades this formation of antisite defects has been investigated with ^{27}Al nuclear magnetic resonance (NMR) where the major central transition peak represents Al species on regular octahedral AlO_6 sites whereas a secondary peak shows the concentration of displaced Al on tetrahedral AlO_4 positions. A first application of this technique to the laboratory-designed spinels (A) and (B) confirmed an expected and reasonable feature [9]: spinel (A) built on a pre-existing cubic template lattice (of MgO particles) exhibits a significantly lower concentration of disordered Al species (about 0.175 referred to all Al; $i = 0.35$) compared with a higher cation disorder (~ 0.205 of disordered Al; $i = 0.41$) in spinel (B) which was built *ab initio*. This finding explains the lower sintering temperature of the disordered spinel (B) because increasing cation inversion in stoichiometric spinel is associated with trimer Schottky defect clusters which include vacancies of oxygen [5] as the biggest and, therefore, slowest diffusing species [10].

Thus, this previous study [9] enabled robust experimental evidence with an important insight: At equal stoichiometric composition and, after equal calcination with equal particle sizes and with equal pore size distributions (i.e. equal homogeneity of particle coordination) in the green bodies, a higher cation disorder of $i = 0.41$ vs $i = 0.35$ can initiate a significant decrease in the sintering temperature of high-purity spinel by about 200 °C.

With this fundamental evidence from tests with laboratory-synthesized spinel powders it was the objective of the present study to ascertain whether this effect is also significant in commercial raw spinel powders. Another target was to determine the crystallographic reproducibility of commercial syntheses.

II. Experimental

Table 1 shows typical chemical and granulometric data of the investigated commercial spinel powder products. Flame spray pyrolysis and alum process spinel exhibit similar specific surfaces (~ 30 m^2/g) and particle sizes (50 – 60 nm), the third powder was coarser (~ 120 nm). Size distributions with a slightly worse dispersibility of the alum process spinel and high resolution micrographs of these powders have been published previously [8]. All molar compositions $MgO:Al_2O_3$ were close to 1:1.

Table 1: Commercial high-purity $MgAl_2O_4$ spinel powders from different syntheses.

Synthesis	Flame Spray Pyrolysis [USA]	Alum Process [F]	Thermal Decomposition with Ammonium Carbonate [J]
Purity	~ 99.995 % spinel [10 – 20 ppm Fe]	~ 99.995 % spinel [~ 15 ppm Fe]	~ 99.995 % spinel [6 – 8 ppm Fe]
Specific BET surface, equivalent particle size	30 – 33 m^2/g 50 – 60 nm	28 – 30 m^2/g 50 – 60 nm	13 – 17 m^2/g 110 – 130 nm

Samples for sintering experiments were prepared by means of de-agglomeration milling with an additive of about 4 % organic binders, freeze drying, uniaxial pre-pressing at about 50 MPa and subsequent cold isostatic pressing at 700 MPa. No sintering additives were used in order to investigate the original sintering ability of the powders without secondary influences. With a previously described approach [3] an optimum homogeneity of the particle coordination in the green state was controlled by measuring the pore size distributions of samples after outgassing at 800 °C [8]. Additionally, green densities were measured geometrically and checked based on the total intrusion volume of mercury porosimetry. These data together with the wide range of recorded pore sizes (6 – 500 nm) enabled a reliable assessment of homogeneous or aggregated particle coordinations which may influence the sintering densification. All sintering experiments started with green samples that exhibited similar green densities of $58^{\pm 3}$%.

After burnout of organic additives all samples underwent pressureless pre-sintering up to closed porosity (> 95...98 % of relative density) followed by hot isostatic pressing (HIP) in argon for 15 h at 200 MPa. All samples were pre-sintered in air because preliminary experiments did not reveal systematic differences of the final density or of the achieved transmission depending on the atmosphere (air or vacuum).

Solid-state ^{27}Al MAS-NMR (magic-angle spinning nuclear magnetic resonance spectroscopy) of spinel powders was performed with an Avance^{TM} 400MHz WB spectrometer (Bruker-Biospin, Karlsruhe, Germany) operating at 104.29 MHz for ^{27}Al using a 4-mm rotor at a spinning speed of 15 kHz. Spectra were referenced to 1M aqueous $AlCl_3$ = 0 ppm. For quantification, excitation pulses were chosen < 15°, 2000 scans were accumulated with a repetition time of 1 s. Owing to the fact that the AlO_4 and AlO_6 environments were separated to > 98 %, their ratio could be determined by simple integration. The validity of this attempt was checked for one sample by integration and deconvolution of the quadrupolar line shapes giving values differing by less than 2 %, which is within the range of the experimental error.

Plots of the conventionally measured relative density versus the temperature describe the sintering densification sufficiently accurately for early and intermediate sintering stages. The density of such sintered parts was measured based on the Archimedes' principle with a careful record of the temperature of the deionized and deaerated water.

Differences in final-stage sintering (with elimination of last 10^{-4} of residual porosity for achieving transparency) were recorded by measuring the in-line transmittance of sintered, ground and polished disks. This transmission is diminished by scattering losses that depend, however, not only on the porosity but also on the ratio of the size of the pores to the applied wavelength: For 1-mm-thin spinel with 0.01 % porosity, only the in-line transmission of short UV wavelengths of e.g. 200 nm is a sufficiently sensitive measure responding to all pore sizes that commonly exist in transparent microstructures (with the biggest effect by pore sizes close to the wavelength); at larger wavelengths the scattering power of pores diminishes and makes e.g. IR light inappropriate for a record of smaller pores in thin samples [9]. Even at infrared wavelengths, however, only thin windows tolerate pores < 100 nm without a significant loss of transmission. Thus, the most sensitive check for last small pores is in-line transmission through thicker windows at shorter wavelengths. Therefore, for relative densities > 99.9 % the success of sintering was assessed based on the real in-line transmission (RIT) of ~ 4-mm-thick polished disks measured with an aperture of ~ 0.5 ° (LCRT 2000 Gigahertz Optics) at 640-nm wavelength (Fig. 1). This measurement excludes scattered light that is included in "in-line" data of commercial spectrometers with larger effective apertures of 3 – 5° [11, 12].

III. Results and Discussion

(1) Flame spray pyrolysis spinel

Fig. 2 gives the ^{27}Al MAS NMR spectrum of two spinel lots obtained by means of flame spray pyrolysis. The major peak of the central transition represents the Al species on "regular" octahedral AlO_6 sites. The smaller peak at about 69 ppm is caused by "disordered" Al on tetrahedral AlO_4 lattice places substituting Mg. As to be expected after highly dynamic flame spray pyrolysis, this lattice exhibits the highest cation disorder of the investigated commercial spinel powders (Table 2).

With its high concentration of antisite defects this lattice could, eventually, be in a metastable state, i.e. with a risk of limited reproducibility. However, NMR spectra of powders from different manufacturing lots revealed a nearly perfect reproduction of all features of the central transition as well as of the satellite transitions (Fig. 2).

Table 2: Cation disorder derived from NMR spectra of differently synthesized commercial $MgAl_2O_4$ spinel powders.

Synthesis →	Flame Spray Pyrolysis (*highly dynamic*)	Alum Process (*static* calcination) typical lots, lot X	*Static* thermal Decomposition with Ammonium Carbonate regular – lot Z
AlO_4/AlO_6	0.22	0.17	0.10 – 0.14
AlO_4/Al_{total}	0.18	0.14	0.09 – 0.12
Inversion parameter *i*	0.36	0.29	0.18 – 0.25

(2) Alum process spinel

After static calcination the alum process powder (with similar particle size as the flame pyrolysis spinel) exhibits a lower degree of cation disorder than the spinel from the highly dynamic flame spray pyrolysis (Fig. 3, Table 2).

The small difference in the fine structure of the AlO_6 peak in Fig. 3 is probably due to the different cation disorder. In "ideal" stoichiometric spinel (without Al on tetrahedral sites) the major peak of the central transition exhibits a second-order quadrupole splitting [13, 14]. Increasing cation disorder gives rise to (i) an increasing distribution of the chemical shift δ and of the quadrupole coupling constant C_q, and (ii) to an underlying second AlO_6-environment associated with AlO_4 sites having different C_q and δ as confirmed by ^{27}Al MQ (multiple quantum) MAS NMR [15]. With increasing cation disorder both effects result in a fading and, finally, loss of the quadrupole splitting of the AlO_6 central transition as already shown in the work of Maekawa *et al.* [15]. Thus, in Fig. 3 the splitting is still visible in the NMR spectrum of the less disordered alum spinel powder (inversion parameter $i = 0.29$) but not in the spectrum of the flame spray pyrolysis spinel ($i = 0.36$ - Table 2).

Turning to the supposed influence of different cation disorder on the observed sintering and HIP temperatures for complete pore elimination (indicated by similarly high RIT in Fig. 1) we can establish that the difference of the cation disorder in flame spray pyrolysis and in alum spinels ($i = 0.36$ vs. $i = 0.29$) is as big as reported in the introduction for the laboratory-synthesized spinel powders (A) and (B) that exhibited a difference of about 200 °C in their sintering temperatures at equal particle size distribution, specific surface and green body homogeneity [9]. Thus, the difference of cation inversion observed here for flame spray pyrolysis and for alum spinels is sufficiently strong to initiate the different sintering temperatures of these commercial powders displayed in Fig. 1.

On the other hand, we must not neglect the small but significant difference of powder dispersibility and of the homogeneity of green bodies prepared by means of flame spray pyrolysis and of alum process spinels [8].

Summarizing it is, therefore, concluded that both the different cation disorder of flame spray pyrolysis and alum process spinels and their different dispersibilities contribute to their different sintering temperatures in Fig. 1.

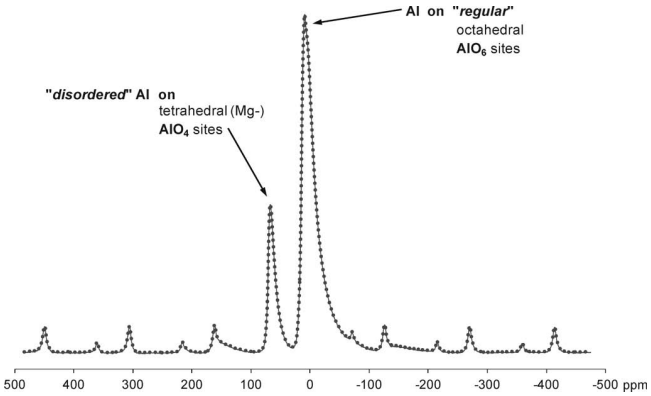

Fig. 2: Reproducibility of the real structure of the spinel lattice by flame spray pyrolysis. The solid line shows the NMR spectrum of a typical manufacturing lot, the dots represent another individual manufacturing batch.

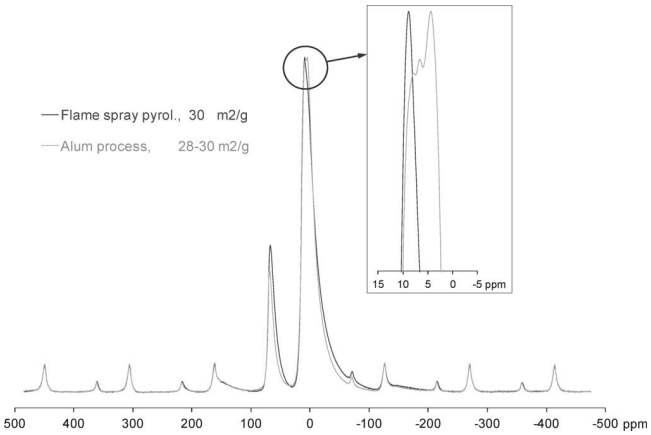

Fig. 3: Comparison of typical NMR spectra of spinel powders from flame spray pyrolysis and from the alum process.

The question of the reproducibility of the alum process synthesis was raised by experiments conducted by A. Goldstein: For a manufacturing lot , he observed a shift of the sintering curve towards higher temperatures and an upper limit of ~ 98.5 % for final pressureless densification (Fig. 4a). The same lot X was used by IKTS Dresden for larger samples [8] which required different processing with about 35 °C higher sintering temperatures (Fig. 4a). For this lot the Dresden tests did not confirm an upper limit of the relative density < 99 % as suggested by Goldstein's results. At lower sintering stages, however, with Dresden processing, lot X exhibited a similar shift towards higher temperatures as observed by Goldstein. Since the specific surface of lot X did not differ significantly from former manufacturing batches, the question was whether a differ-

ence in the real structures of the lattices could be responsible for the observed change in the sintering behavior.

Up until now the NMR results have not given a clear answer: Fig. 4b shows nearly identical cation disorder in the NMR spectra of a typical alum process spinel and of lot X with small differences only in the fine structure of the AlO_6 central transition. Although there is no significant difference in the AlO_4/AlO_6 disorder of these lots, the slightly different fine structure may indicate a small change in the octahedral AlO_6 environments. It is, however, impossible to conclude if a specific change in the lattices has caused the differences in the sintering densification as shown in Fig. 4a.

This uncertainty does not, however, eliminate the surprising experimental experience of Fig. 2 and Fig. 4 that the reproducibility of the static alum process powder is not as perfect as observed for the highly dynamic flame spray pyrolysis.

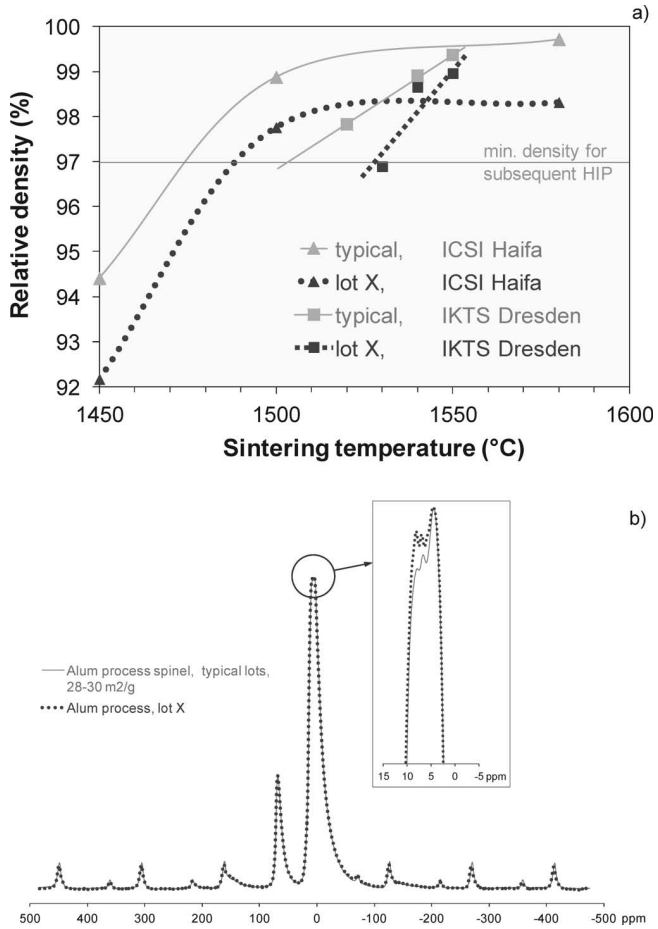

Fig. 4: a) Air sintering of different manufacturing lots of alum process spinel; b) NMR spectra of different manufacturing lots of alum process spinel.

(3) Spinel by thermal decomposition with ammonium carbonate

It is a special advantage of this coarser spinel powder that it can be processed by means of gel-casting and enables, by this means, improved optical homogeneity of thicker components (up to several centimeters!) for larger optical lenses [8] even though gel-casting does not reduce the sintering temperature of this spinel as observed with Al_2O_3 [16]. As a consequence of typical sintering temperatures ~ 1545 °C for this powder (Fig. 1), average grain sizes of HIP-ed transparent microstructures are about 5 – 7 and up to 10 μm [8].

Unlike the not always perfect reproducibility of alum process spinels (Fig. 4), powders from the process with ammonium carbonate exhibited significant deviations only when an intentionally modified batch was manufactured on special request of the present author (A.K.). This batch labeled "lot Z" in Table 2 and Fig. 5a exhibited a significantly lower sintering temperature of ~ 1450 °C for pore closure. Obviously, the improved sintering densification of this lot can neither be explained by the slight unintentional increase in its average particle size nor is it possible to blame the only slightly higher specific surface of regular lots for a possible deterioration of the homogeneity of green bodies as a cause of their higher sintering temperature: the measured pore size distribution of the regular-grade green bodies confirmed an excellent homogeneity with $d_{50}^{pores} \sim 30$ nm (~ $^1/_4$ of the median particle size). Once more, NMR provided the explanation for the improved sintering in full agreement with the observations made with the other commercial spinel powders and with the previous study [9] of laboratory-synthesized grades:

- In Fig. 5b and Table 2 it is the "lot Z" with the higher cation disorder ($i = 0.25$) for which Fig. 5a shows the lower sintering temperature.
- Again this higher cation disorder is associated with fading quadrupole splitting of the central transition (Fig. 5b).

Regarding the special binding situation of lattice species in surfaces it is not surprising that the literature presents experimental indications that the degree of cation inversion may scale with the surface area of spinel powders [17, 18]. The size of this influence and its dependence on manufacturing conditions is, however, not clear. Here, it is interesting to note the close values of cation inversion measured for "lot Z" of the spinel synthesized with ammonium carbonate ($i = 0.25$) and for the alum process spinel ($i = 0.29$). Since the specific surfaces of these powders differ by more than a factor of two, it appears that the degree of cation disorder depends on the chemical and thermal history, but is not largely influenced by size and surface curvature of the particles.

IV. Summary and Conclusions

A previous study with laboratory-synthesized high-purity stoichiometric spinel powders enabled experimental evidence of a strong impact of the degree of cation disorder on the sintering performance at constant particle size and homogeneity of green shaped bodies [9] and was extended here to commercial high-purity spinel powders. The new results confirm that significant profit can be achieved by successful integration of low-defect processing with an improved control of the real structure of the spinel lattices:

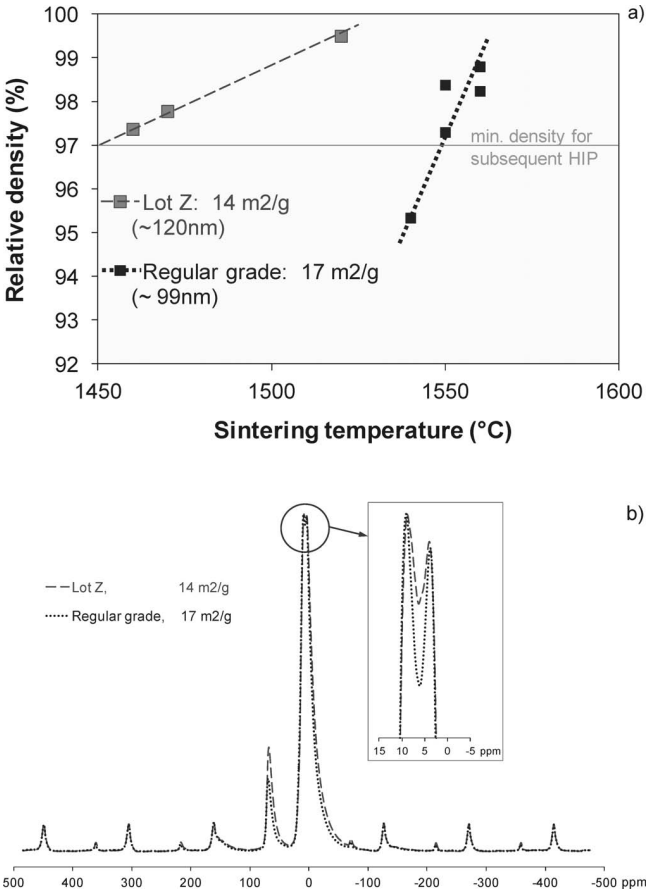

Fig. 5: a) Air sintering of different manufacturing lots of spinel powders obtained by thermal decomposition with ammonium carbonate; b) NMR spectra of spinel powders obtained by thermal decomposition with ammonium carbonate.

(1) Cation inversion depending on powder synthesis

Highly dynamic flame spray pyrolysis gives spinel with the highest degree of cation disorder (inversion parameter $i = 0.36$). A lower inversion ($i = 0.29$) is observed for similarly fine but statically calcined alum process spinel. The lowest cation disorder ($i = 0.18$) is recorded for regular grades of commercial spinel prepared with thermally decomposed ammonium carbonate. This synthesis gives coarser powders manufactured, probably, by higher calcination. The low inversion of these powders compares, therefore, with previous records of a moderately lower cation disorder in dense ceramics that were subject to higher sintering and HIP temperatures [9].

In contrast to the obvious influences of the chemical and thermal history the investigations did not show a large impact of the size of the spinel particles on the observed degree of cation disorder.

(2) Reproducibility of spinel syntheses

The NMR spectra of different manufacturing lots of flame spray pyrolysis spinel indicate a perfect reproducibility within the frame of this synthesis.

The fine structure of NMR peaks of alum process spinel powders is not exactly reproduced by nominally equal manufacturing lots which sometimes also exhibit deviations in their sintering performance.

(3) Impact of cation inversion on sintering densification

By comparison with laboratory-synthesized powders it could be shown that the high cation disorder of flame spray pyrolysis spinel contributes significantly to its low sintering and HIP temperatures about 200 °C below the temperatures needed for alum process spinel powders with similar specific surface.

Similarly, experiments with spinel synthesized with ammonium carbonate showed that the sintering temperature required for a closure of pores in green bodies (as a prerequisite for subsequent cladless HIP) can be reduced by about 100 °C when the synthesis is modified in a way that increases the cation disorder from the regular-grade inversion $i = 0.18$ up to $i = 0.25$.

(4) Cation disorder and quadrupolar peak splitting

Quadrupolar splitting of the main peak of the central transition is a typical feature in ideal spinel ($i = 0$). Our experiments confirm a fading and final loss of this fine structure at increasing cation disorder as reported by Maekawa *et al.* [15] owing to an increasing distribution of C_q and δ in addition to an overlapping second AlO_6 component. This splitting does not indicate an independent structural issue but appears to be associated with the degree of cation disorder.

Acknowledgements

The green samples for the present investigation were processed and sintered by T. Hutzler at IKTS Dresden. The sintering data for samples made of alum process spinel lot X and processed by ICSI Haifa (Fig. 4a) were kindly provided by Dr. A. Goldstein from the Israel Ceramic and Silicate Institute, Haifa.

References

1 Krell, A., Blank, P.: The influence of shaping method on the grain size dependence of strength in dense submicrometre alumina, *J. Eur. Ceram. Soc.*, **16**, 1199 – 1200, (1996).

2 Krell, A., Klimke, J., Hutzler, T.: Advanced spinel and sub-μm Al_2O_3 for transparent armour applications, *J. Eur. Ceram. Soc.*, **29**, 275 – 281, (2009).

3 Krell, A., Klimke, J.: Effect of the homogeneity of particle coordination on solid state sintering of transparent alumina, *J. Am. Ceram. Soc.*, **89**, 1985 – 1992, (2006).

4 Krell, A., Hutzler, T., Klimke, J.: Transmission physics and consequences for materials selection, manufacturing, and applications, *J. Eur. Ceram. Soc.*, **29**, 207 – 21, (2009).

5 Ball, J.A., Murphy, S.T., Grimes, R.W., Baconrisen, R.W., Smith, R., Uberuaga, B.P., Sickafus, K.E.: Defect processes in $MgAl_2O_4$ spinel, *Solid State Sci.*, **6**, 717 – 724, (2008).

6 Schmocker, U., Waldner, F.: The inversion parameter with respect to the space group of $MgAl_2O_4$ spinels, *J. Phys. C: Solid State*, **9**, L235 – L237, (1976).

7 Fischer, P.: Neutron diffraction of $MgAl_2O_4$ and $ZnAl_2O_4$ spinel structures depending on their thermal history (in German), *Z. Kristallog.*, **124**, 275 – 302, (1967).

8 Krell, A., Hutzler, T., Klimke, J., Potthoff, A.: Fine-grained transparent spinel windows by the processing of different nanopowders, *J. Am. Ceram. Soc.*, **93**, 2626 – 2666, (2010).

9 Krell, A., Waetzig, K., Klimke, J.: Influence of the structure of $MgO{\cdot}nAl_2O_3$ spinel lattices on transparent ceramics processing and properties, *J. Eur. Ceram. Soc.*, **29**, 2887 – 2898, (2012).

[10] Bratton, R.J.: Initial sintering kinetics of $MgAl_2O_4$, *J. Am. Ceram. Soc.*, **52**, 417 – 419, (1969).

[11] Apetz, R., Van Bruggen, M.P.B.: Transparent alumina: a light scattering model, *J. Am. Ceram. Soc.*, **86**, 480 – 486, (2003).

[12] Yamamoto, H., Mitsuoko, T., Iio, S.: Translucent polycrystalline ceramic and method for making same, Europ. Patent Application EP - 1 053 983, (2000).

[13] Brun, E., Hafner, S.: The electric quadrupole splitting of Al^{27} in spinel $MgAl_2O_4$ and corundum Al_2O_3: I. Paramagnetic nuclear resonance of Al^{27} and cation distribution in spinel (in German), *Z. Kristallog.*, **117**, 37 – 62, (1962).

[14] Behrens, H.-J., Schnabel, B.: The second order influence of the nuclear quadrupole interaction on the central line in the NMR of quadrupolar nuclei using rapid sample spinning, *Physica* 114B, 185 – 190, (1982).

[15] Maekawa, H., Kato, S., Kawamura, K., Yokokawa, T.: Cation mixing in natural $MgAl_2O_4$ spinel: A high-temperature ^{27}Al NMR study, *Am. Mineral.*, **82**, 1125 – 1132, (1997).

[16] Krell, A., Blank, P., Ma, H., Van Bruggen, M., Apetz, R.: Transparent sintered corundum with high hardness and strength, *J. Am. Ceram. Soc.*, **86**, 12 – 18, (2003).

[17] Šepelák, V., Indris, S., Heitjans, P., Becker, K.D.: Direct determination of the cation disorder in nanoscale spinels by NMR, XPS, and Mössbauer spectroscopy, *J. Alloy. Compd.*, **434/435**, 776 – 778, (2007).

[18] Rasmussen, M.K., Foster, A.S., Hinnemann, B., Canova, F.F., Helveg, S., Meinander, K., Martin, N.M., Knudsen, J., Vlad, A., Lundgren, E., Stierle, A., Besenbacher, F, Lauritsen, J.V.: Stable cation inversion at the $MgAl_2O_4$ (100) surface, *Phys. Rev. Lett.*, **107**, 036102/1 – 4, (2011).